Control of DFIG based Wind Generation to Improve Inter-Area Oscillation Damping

Zhixin Miao, *Member, IEEE*, Lingling Fan, *Member, IEEE*, Dale Osborn, *Member, IEEE*, Subbaraya Yuvarajan, *Senior Member, IEEE*

Abstract—**Power systems with high penetration of wind power usually require long-distance transmission to export wind power to the market. Inter-area oscillation is an issue faced in long distance transmission. Can wind generation based on doubly fed induction generator (DFIG) help to damp oscillations and how? In this paper, a control scheme is developed for the DFIG with rotor side converter to damp inter-area oscillations. The DFIG is modeled in Matlab®/Simulink utilizing its vector control scheme feature, and inner current control and outer active/reactive power control loops are modeled and designed. A two-area system that suffers from poor inter-area oscillation damping along with a wind farm in the area that exports power is investigated. A damping controller is designed and time-domain simulations are used to demonstrate the effectiveness of the controller. The major contributions of the paper are as follows: 1) Built a wind farm inter-area oscillation study system based on the classical two-area four-machine system, 2) Established that in vector control scheme, active power modulation can best help to damp oscillations, 3) Successfully designed a feedback controller using remote signals with good inter-area oscillation observability.**

Index Terms—**Wind Generation, Doubly Fed Induction Generator, Inter-Area Oscillation**

I. Introduction

THE demand for renewable energy increases day by day for the apparent concerns of energy shortage and global warming. In Europe and US, legislative acts have been enforced for the increased usage of renewable energy. Wind generation is one type of renewable energy resource that has been the focus of renewable energy profile in states with strong wind resources. California and Texas are the leading states to use wind energy and other states follow up. In Minnesota, it is recommended that the renewable power penetration be increased to 25% by 2025 [1].

Based on the electrical topology, wind turbine generators can be classified into the following four categories: [2]:

1) fixed-speed squirrel-cage induction generators,
2) variable-slip (wound rotor) induction generators with variable rotor resistance,
3) variable-speed doubly fed asynchronous generators, and
4) variable-speed generators with full converter interface.

Compared to a fixed-speed wind generator, the key advantages of the variable-speed generator are (a) its ability to extract maximum electric power at various wind speeds

Z. Miao and D. Osborn are with transmission asset management department, Midwest ISO Inc, St. Paul MN 55108. email: Zhixin.Miao@ieee.org, DOsborn@midwestiso.org

L. Fan and S. Yuvarajan are with Dept. of Electrical & Computer Engineering, North Dakota State University, Fargo, ND 58105. Email: Lingling.Fan@ndsu.edu, Subbaraya.Yuvarajan@ndsu.edu.

via rotor speed adjustment and (b) reduced mechanical stress imposed on the turbine. On the other hand, the fixed-speed generator maintains a constant rotor speed. Though it requires simple power electronics interface, the fixed speed induction generator has a low efficiency of wind power conversion and no ability to provide reactive power support. It also imposes tense mechanical stress on the turbine and requires complex pitch control to maintain a constant rotor speed [3].

The doubly fed induction generator (DFIG) is a popular type of variable speed generator used in wind generation. Large wind farms are usually located at remote areas and long distance transmission is involved in getting wind power to the market. With long distance transmission, oscillations and especially inter-area oscillations limit the power transfer capability. When the penetration of DFIG-based wind generation is significant, the damping of oscillations by controlling the DFIG becomes an important issue to be addressed. Hughes *et al* [4] used a Power System Stabilizer (PSS) in a DFIG with a rotor-side converter to damp power system oscillations. The control is based on Flux Magnitude and Angle control (FMAC) where the rotor flux magnitude controls the reactive power/voltage while rotor flux angle controls the active power/torque. The test system constructed in [4] does not exhibit inter-area oscillation phenomenon. Since the stator voltage-oriented or flux-oriented vector control is used widely in DFIG [3], [5], the investigation of the oscillation damping capability in vector control based DFIG is of practical value. Researches have not addressed the inter-area oscillation problems caused by high penetration of wind generation. In [6], the DFIG penetration was added to the classic inter-area oscillation test system. The authors have investigated the function of a supplementary damping control loop added at rotor voltage point.

The objective of this paper is to develop a control strategy that can effectively damp inter-area oscillations in a power system. In addition, a full-order model in Matlab®/Simulink is presented for the DFIG with vector-control based current-control loops and active and reactive power control loops. A supplemental signal containing the inter-area oscillation information will be introduced into the control loops to enhance the system damping. In this paper, decoupled vector control schemes and control loops are modeled including more details. The inner current control loops are also included. Active power modulation and reactive power modulation are investigated for their effectiveness on inter-area oscillation damping. The complete design of the damping controller design is presented.

The paper is organized as follows: Section I is the introduction and it contains the research objective of the paper.

Section II describes the DFIG model and vector control concept. Section III presents the configuration of the test system. Section IV presents the control loops and the control strategy for damping inter-area oscillations through DFIG with rotor-side converter. The difficulties involved in the design are also presented. Section V presents the simulation results and discussion. Section VI concludes the paper.

II. DFIG MODEL AND VECTOR CONTROL CONCEPT

In this section, the dynamic model of the DFIG is presented by a set of mathematical equations. The configuration of a grid-tied system with a DFIG and wind turbine is shown in Fig. 1. The stator of the DFIG is connected to the grid with voltage v_s and current i_s. The grid in turn supplies injection power to the rotor through a set of PWM converters.
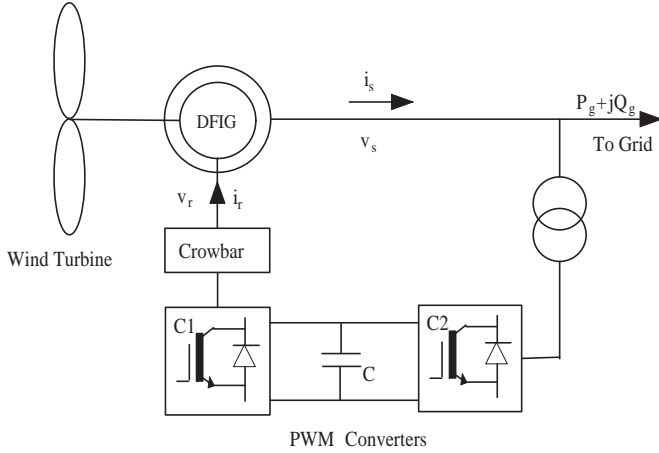

Fig. 1.   Grid-tied DFIG wind turbine system.

The DFIGs are wound-rotor induction generators with rotor windings into which variable frequency (ω_{v_r}), variable magnitude AC voltages can be injected. This AC voltage will generate a flux linkage with a frequency ω_{v_r} if the rotor is stand still. When the rotor is rotating at a speed ω_r (due to the wind turbine), the net flux linkage generated by the rotor with the injected voltage will have a frequency $\omega_r + \omega_{v_r}$ [3]. The net flux linkage will be kept constant at 60 Hz at various wind speeds by adjusting the injection frequency. In this study, the time frame of analysis (oscillation) is restricted to 20 seconds. It is reasonable to assume that the wind speed remains constant during this period and the mechanical torque is also constant.

The stator and rotor voltage equations of an induction machine are written in the following matrix form:

$$\underline{v}_{abcs} = r_s\underline{i}_{abcs} + \frac{d\underline{\lambda}_{abcs}}{dt} \tag{1}$$

$$\underline{v}_{abcr} = r_r\underline{i}_{abcr} + \frac{d\underline{\lambda}_{abcr}}{dt}. \tag{2}$$

The voltage equations of an induction machine in the arbitrary reference frame (d-q) can be written in terms of the currents as [7], [8]:

$$\underline{v}_{dqs} = r_s\underline{i}_{dqs} + \frac{d\underline{\lambda}_{dqs}}{dt} + \omega_e \times \underline{\lambda}_{dqs} \tag{3}$$

$$\underline{v}_{dqr} = r_r\underline{i}_{dqr} + \frac{d\underline{\lambda}_{dqr}}{dt} + (\omega_e - \omega_r) \times \underline{\lambda}_{dqr} \tag{4}$$

where ω_e is the speed of the synchronously rotating reference frame, and ω_r is the rotor (shaft) speed. The model of a wound-rotor induction generator is different from that of a squirrel cage induction generator in which v_{qr} and v_{dr} are zero. In the case of a DFIG, the two variables v_{qr} and v_{dr} are controllable via the rotor side inverter. The torque developed can be expressed as

$$T_e = \frac{3}{2}\frac{p}{2}(\lambda_{qm}i_{dr} - \lambda_{dm}i_{qr}) \tag{5}$$

where $\lambda_{qm} = \lambda_{qs} - i_{qs}L_{ls}$ and $\lambda_{dm} = \lambda_{ds} - i_{ds}L_{ls}$. λ_{qm} and λ_{dm} are called the q-axis and d-axis air gap flux linkages.

To obtain a constant stator frequency ω_e, the sum of the frequency of the injected rotor voltage or current ω_{v_r} and the frequency of the rotor (proportional to shaft speed) ω_r should equal ω_e giving

$$\omega_e = \omega_{v_r} + \omega_r. \tag{6}$$

In the voltage equations (3) and (4), if we ignore the leakage resistance of the stator, it can be found that under steady state, v_{ds} will be in phase with λ_{qm} while v_{qs} will be in phase with λ_{dm}. If $v_{ds} = 0$, then $\lambda_{qm} = 0$. Therefore, the alignment of the q-axis with v_s is the same as the alignment of the air gap flux with the d-axis of the reference frame.

The torque equation is now reduced to

$$T_e = \frac{3}{2}\frac{p}{2}\lambda_{dm}i_{qr} \tag{7}$$

and the reactive power Q_s can be expressed in terms of the rotor current as [8]

$$Q_s = \frac{3}{2}\omega_e\left(\frac{L_s\lambda_{dm}^2}{L_m^2} - \lambda_{dm}i_{dr}\right). \tag{8}$$

From the expressions for the torque and reactive power, it can be seen that the rotor currents can independently control real and reactive power. The rotor currents can in turn be controlled by the injected rotor voltage. The current i_{qr} will be controlled by v_{qr} and i_{dr} will be controlled by v_{dr}. Thus, we can control the active power by controlling v_{qr} and reactive power by controlling v_{dr}.

III. CONFIGURATION OF TEST SYSTEM

The test system shown in Fig. 2 is based on the classic two-area four-machine system developed in [9] for inter-area oscillation analysis. Area 1 has two synchronous generators, each with 835 MW rated power and Area 2 also has two synchronous generators, each with 835 MW rated power. All four synchronous generators are identical. In this paper, the full-order model of the synchronous generators is used. The parameters of the steam turbine generators come from Krause's classic textbook *Analysis of Electric Machinery* [7]. The parameters are also shown in Table I of Appendix. In Area 1, a wind farm is connected to the grid. The wind farm penetration is assumed to be 25% of Area 1, *i.e.*, the rated exporting power level of the wind farm is 200 MW.

The transfer level along the tie line of the two areas varies from 0 MW to 400 MW due to the variation of load levels in the two areas. The inter-area oscillation is characterized as the swing of the generators in Area 1 against the generators
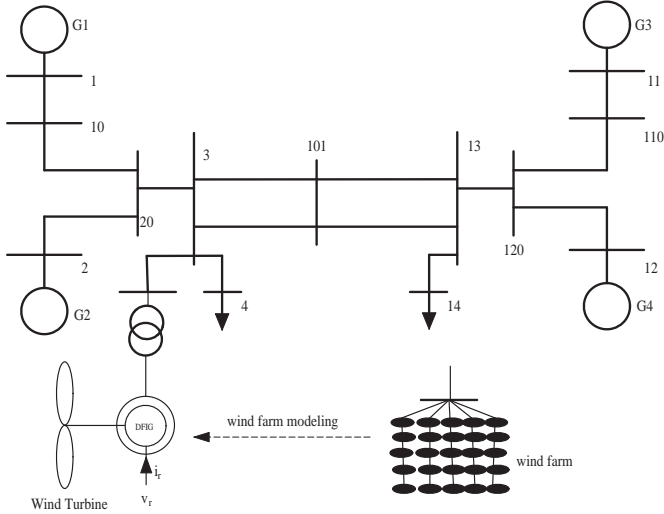
Fig. 2. One-line diagram of two-area system with wind generator.

Fig. 3. Bode diagram of i_{qr}/v_{qr}.

in Area 2 and the frequency of the oscillation is about 0.7 Hz or 4.35 rad/s. In addition, there are local oscillations present in the system at about 7.7 rad/s. The local oscillations are characterized as the swing of one synchronous generator against the other in the same area.

IV. CONTROL OF DFIG

In this section, the control loops around the rotor-side converter of a DFIG are discussed in detail. The DFIGs rotor-side control usually consists of the inner current control loop, and outer loops for active and reactive power control. This type of control structure is also called cascade control and is widely used in inverter control of induction machines [10]. The control loops can be designed independently since the bandwidth of the current control loop is much higher than those of the outer loops.

A. Inner Current Control Loop of DFIG

The inner current control loop senses the rotor currents and feeds back suitable rotor voltages. From the voltage equations expressed in (3) and (4), the state space model can be obtained as [6]:

$$\frac{d}{dt} \begin{bmatrix} i_{qs} \\ i_{ds} \\ i_{qr} \\ i_{dr} \end{bmatrix} = A(\omega_e, \omega_r) \begin{bmatrix} i_{qs} \\ i_{ds} \\ i_{qr} \\ i_{dr} \end{bmatrix} + B(\omega_e, \omega_r) \begin{bmatrix} v_{qs} \\ v_{ds} \\ v_{qr} \\ v_{dr} \end{bmatrix}. \tag{9}$$

Two PI controllers, one from i_{qr} to v_{qr} and the other from i_{dr} to v_{dr} are used to track the reference rotor current.

The DFIG has a natural oscillation mode of about 60 Hz and a higher-than 60 Hz bandwidth for the loop means a fast response. The PI controllers are to be designed to have a 100 Hz gain crossover frequency and a 90 degree phase margin [11]. The open loop frequency responses of the DFIG are plotted in Figs. 3 and 4.

The plant has a transfer function $G(s)$ and its frequency response at ω_c is $G(j\omega_c)$. Assume a PI controller with
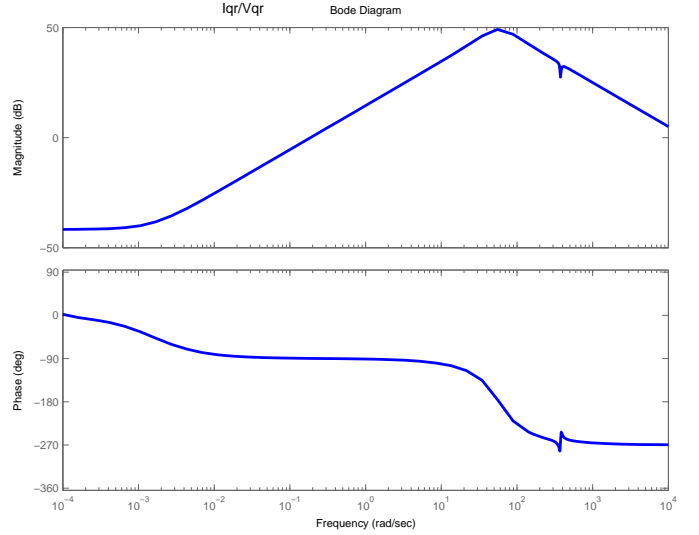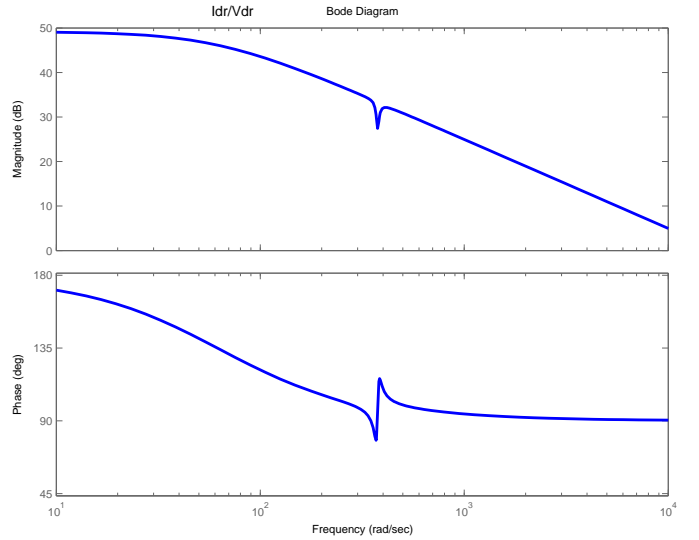

Fig. 4. Bode diagram of i_{dr}/v_{dr} relation.

$C(s) = K_p + \frac{K_i}{s}$ and its response at the crossover frequency ω_c becomes $C(j\omega_c) = K_p - j\frac{K_i}{\omega_c}$. According to the frequency domain design criteria, the phase margin ϕ of the compensated system is given by [12]

$$C(j\omega_c)G(j\omega_c) = 1\angle(-180 + \phi)^\circ. \tag{10}$$

If $\theta = -180 + \phi - \angle G(j\omega_c)$, then the controller parameters K_p and K_i are given by

$$K_p = \frac{\cos\theta}{|G(j\omega_c)|} \tag{11}$$

$$K_i = \frac{\sin\theta\,\omega_c}{|G(j\omega_c)|}. \tag{12}$$

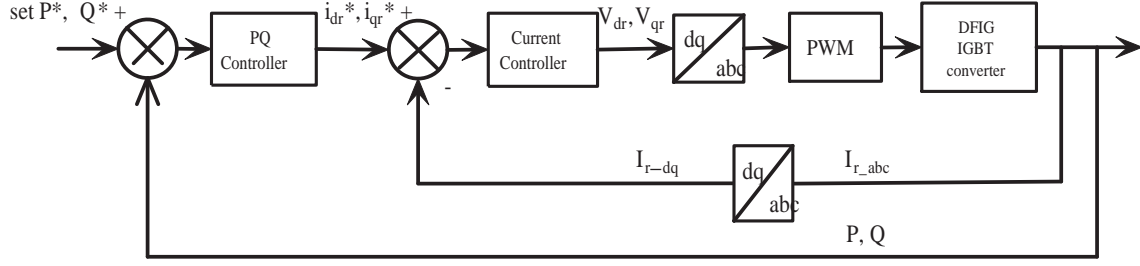The parameters of the PI controllers are shown in the Appendix.

Fig. 5.   Block diagram of PQ tracker.

B. Active Power and Reactive Power Control of DFIG

Federal Energy Regulatory Commission (FERC) Order 661 requires the wind power plants to have the capability to control their reactive power so that the power factor falls within 0.95 leading to 0.95 lagging range [2]. Therefore the capability to track PQ is a basic requirement for a DFIG system. Active power and reactive power (PQ) tracking can be achieved by two PI controllers as shown in Fig. 5. Due to the decoupling nature of vector control, one can adjust v_{qr} based on P and v_{dr} based on Q.

C. Damping Control of DFIG

Since the current loop is very fast and its bandwidth is very high compared to the desired bandwidth of the damping control loop, there is no need to put a supplementary signal at the current control loop. Instead, we propose to add a supplementary signal at the active power control loop. Since the inter-area oscillation is a phenomenon related to the rotor angle and active power, active power modulation is an effective method for damping oscillations in power systems.

The rotor angle difference has a good observability of the inter-area oscillation mode between the two areas [13]. The rotor angle difference can be estimated from local measurements (voltage and current) using the method of [13]. The angle difference signal can be obtained accurately using a state-of-art Phasor Measurement Unit. In this paper, we assume that the angle difference signal is available through either phasor measurement technology or local measurement and estimation.

The open-loop frequency responses of two systems, one with P modulation and a second with Q modulation are compared in Fig. 6. The first system relates the P modulation and the rotor angle difference and the second system relates the Q modulation and the rotor angle difference. It is seen that the oscillation frequency is about 4 rad/s at which the first system has a higher magnitude compared to the second. To control the first system, we will need a smaller gain which is preferred since it avoids controller saturation. Thus the frequency responses confirm that the active power modulation is a good choice for damping inter-area oscillations. The block diagram of the overall system including the controllers and the DFIG with rotor side converter is shown in Fig. 7.

The root locus diagram of the open loop system is shown in Fig. 8. The open loop system is unstable since there are two pairs of complex poles on the right half plane. One pair of poles corresponds to the inter-area oscillation mode at 4.73
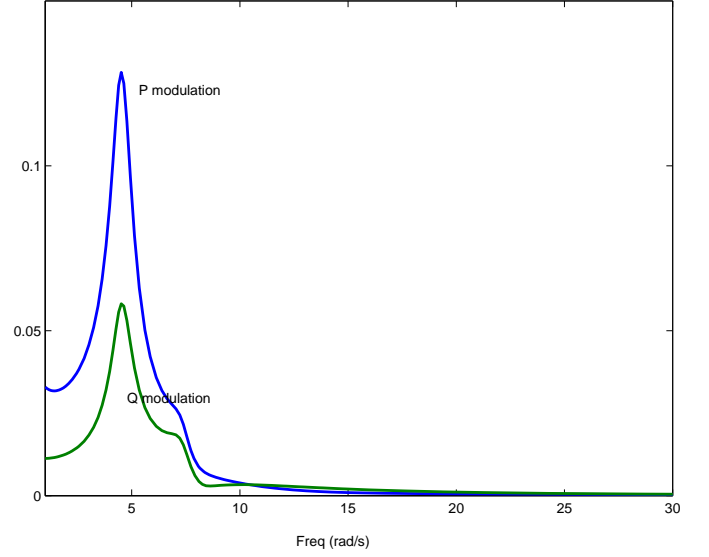

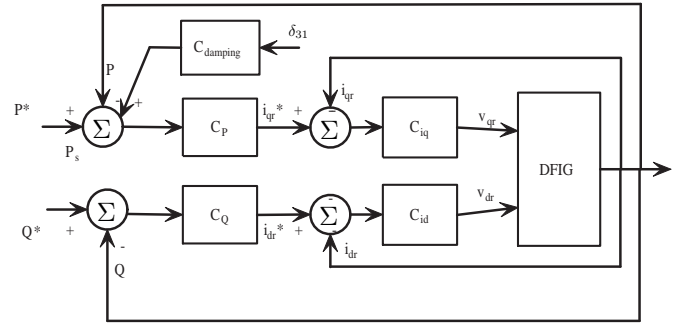Fig. 6.   Open-loop frequency responses with P modulation and Q modulation

Fig. 7.   The overall control structure of the DFIG with rotor side converter

rad/s and the other pair corresponds to an oscillation mode at 7.74 rad/s. The later oscillation mode is a local oscillation mode characterized by one generator oscillating against the other in the same area. The second pair of poles has the associated zeros close-by on the left half plane. Therefore it is impossible to move the second pair of poles to further left. The best option is to move the closed-loop poles as close to the zeros as possible.

A simple proportional controller cannot do the job due to the fact that the two oscillation modes (root locus) will move in opposite directions according to the root locus diagram.
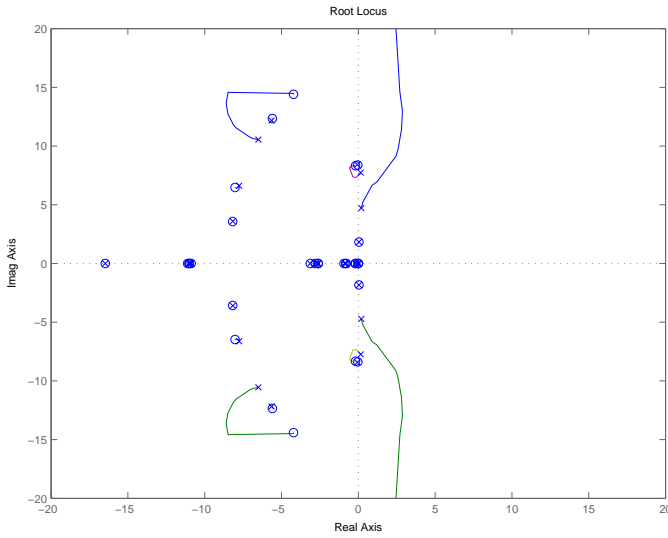
Fig. 8.   Root locus diagram for the open loop system

Moving one mode to the left plane means moving the other mode to the right plane. The order of the open-loop system is high so a more complicated controller is required. The design is simplified by considering the dominant zeros and poles only. The transfer function of the approximate system is given by

$$P = \frac{(s + 0.177 \pm j8.32)(s + 4.22 \pm j14.5)}{(s - 0.209 \pm j4.79)(s - 0.15 \pm j7.67)(s + 6.5 \pm j10.5)}. \tag{13}$$

The frequency response of the approximate system P is compared with that of the original system (Fig. 9). It is seen that the phase angles are the same over the frequency range 1-100 rad/s. However, there are magnitude differences between the two. Compensating P with a gain $k = 0.56$ will make the frequency responses of Pk and the original system the same as shown in Fig. 9.
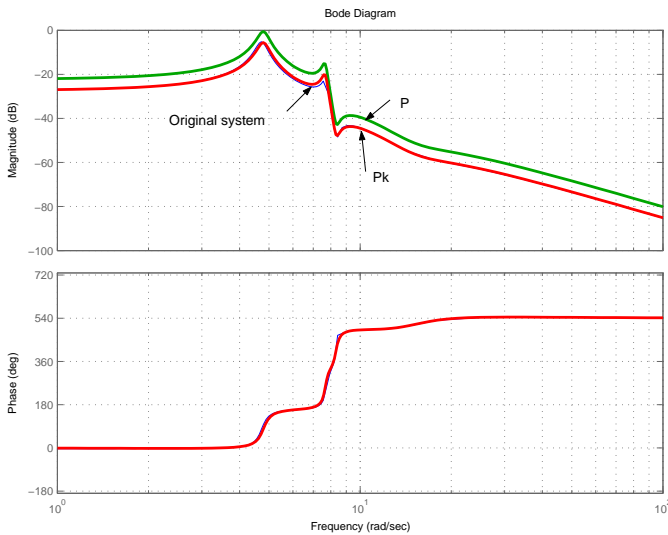

Fig. 9.   Bode plots of the original system and the approximate system

For the approximate lower order system Pk, we now design a controller that can move the two pairs of unstable poles to the

left plane. It is found that the first pair of poles corresponds to the inter-area oscillation mode which has a frequency of 4.73 rad/s. The second pair of the poles corresponds to an oscillation mode with a frequency of 7.74 rad/s. Apparently, the selected input signal (rotor angle difference) is not effective in damping the second oscillation mode since the poles are very close to the zeros. To enhance the damping of the inter-area oscillation mode, a pair of complex zeros ($-0.05 \pm j0.77$, notated as 1 in Fig. 10) is added in the left plane close to the poles. These zeros cause the closed-loop poles move to the left plane when the gain increases. To make the controller proper, two real poles (-6.7,-62.5) on the left real axis are also added. To make the second pair of closed-loop poles move to the corresponding zeros as fast as possible, two pairs of zeros-poles ($-0.62 \pm j6.64$- notated as 2 and $-1.24 \pm j9.01$- notated as 3 in Fig. 10) nearby are added. The controller designed (G_d) is given by

$$G_d = \frac{(1 + 0.17s + 1.3^2 s^2)(1 + 0.028s + 0.15^2 s^2)}{(1 + 0.15s)(1 + 0.016s)(1 + 0.03s + 0.11^2 s^2)}. \tag{14}$$

The root locus diagram of the compensated system kG_dP is also shown in Fig. 10.
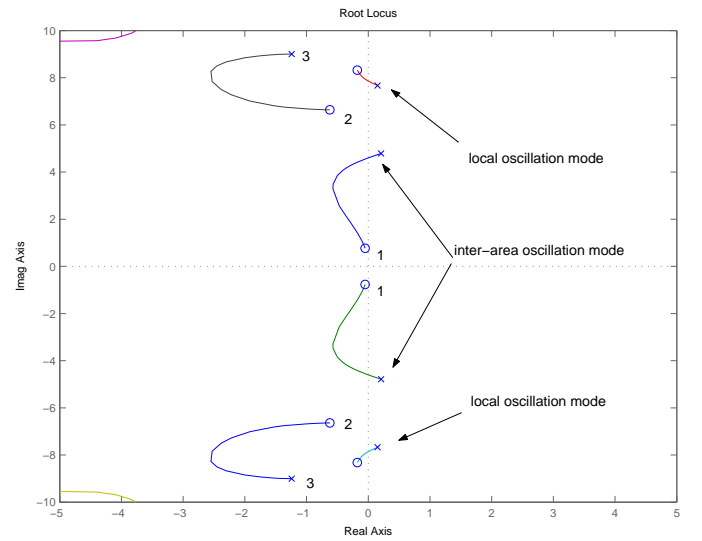

Fig. 10.   Root locus diagram after compensation

The gain that corresponds to maximum damping of the inter-area oscillation mode is computed from the root locus diagram as 2.0. The final damping controller designed is given by

$$C_{damping} = 2\frac{(1 + 0.17s + 1.3^2 s^2)(1 + 0.028s + 0.15^2 s^2)}{(1 + 0.15s)(1 + 0.016s)(1 + 0.03s + 0.11^2 s^2)}. \tag{15}$$

V. SIMULATIONS AND DISCUSSION

Time-domain Simulations are performed on the test system in order to show the effectiveness of the damping control. The system operates under steady state for 0.1 second with the power transfer between the two areas at 400 MW. A temporary three-phase fault occurs at Bus 3 at 0.1 second and is cleared subsequently at 0.1 second. Figs. 11 and 12 show the dynamic

responses of the synchronous generators and the DFIG when there is no inter-area oscillation control. In Fig. 11, the relative angle differences, rotor speeds and electric power export levels are plotted. In Fig. 12, the rotor speed, mechanical torque, electric torque and terminal voltage of the DFIG are plotted. It is seen that the system exhibits low-frequency oscillations whose amplitude increases with time and eventually the system becomes unstable.
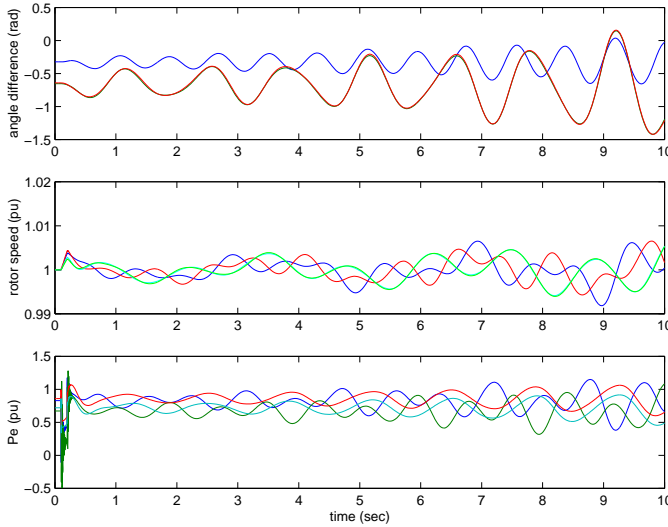

Fig. 11. Synchronous generator dynamic responses with no supplementary damping control. (a) δ_{21}, δ_{31} and δ_{41}, (b) rotor speeds of four generators, (c) output power from generators.
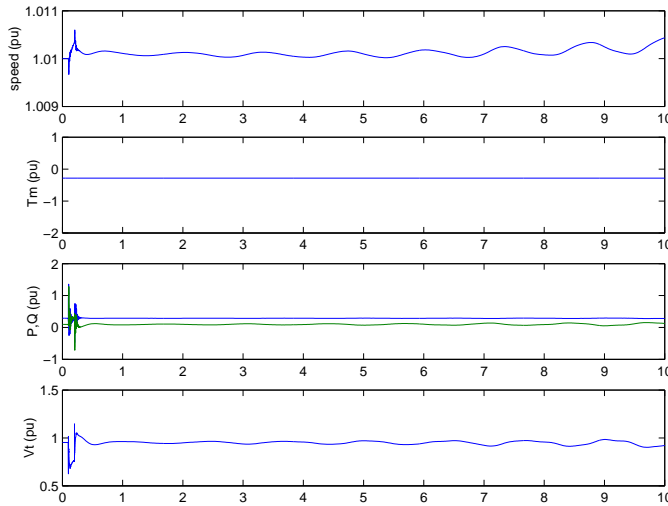

Fig. 12. Wind turbine generation dynamic responses with no supplementary damping control. (a) speed of DFIG rotor, (b) mechanical torque, (c) output P and Q of the DFIG (P is above curve Q), (d) terminal voltage magnitude of the DFIG.

Figs. 13-15 show the dynamic responses of the synchronous generators, the induction generator, and DFIG damping controller with the auxiliary damping control added for active power modulation.

The dynamic responses of the rotor angles are plotted together for the two scenarios: 1) with no damping control,
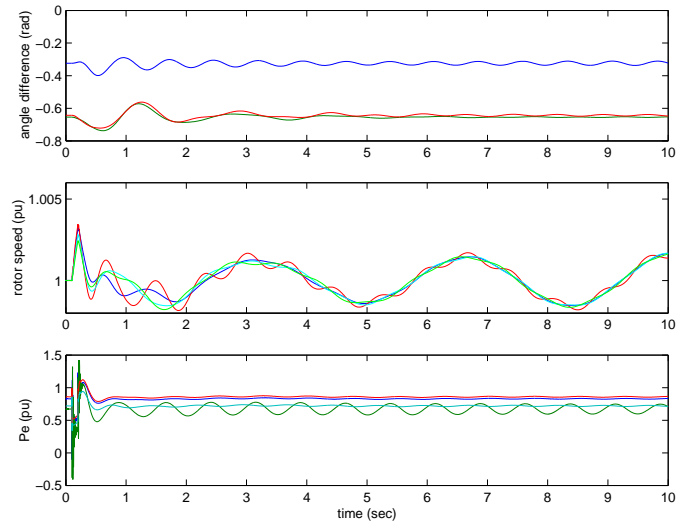

Fig. 13. Synchronous generator dynamic responses with supplementary damping control. (a) δ_{21}, δ_{31} and δ_{41}, (b) rotor speeds of four generators, (c) output power from generators.
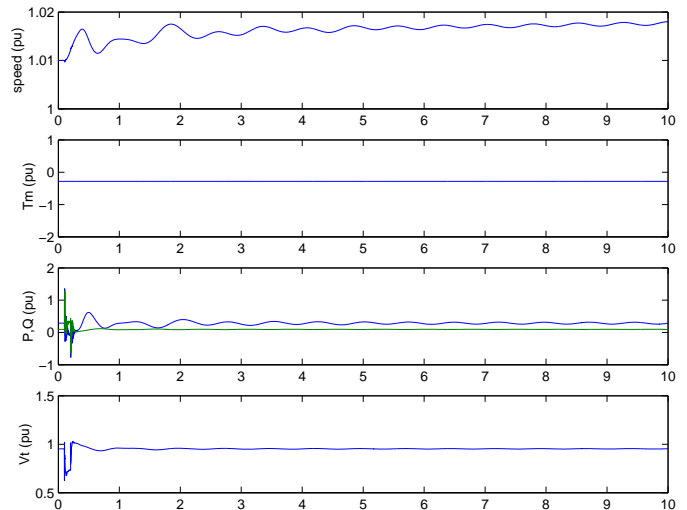

Fig. 14. Wind turbine generator dynamic responses with supplementary damping control. (a) speed of DFIG rotor, (b) mechanical torque, (c) output P and Q of the DFIG (P is above curve Q), (d) terminal voltage magnitude of the DFIG.

and 2) with damping control. The plots are shown in Fig. 16 where dashed lines correspond to the first scenario and the solid lines correspond to the second scenario. From the plots, we can observe the effectiveness of the designed controller in damping out the 0.7 Hz inter-area oscillation. Meanwhile the other oscillation mode tends to damp out as well. Compared to the originally unstable case, the modified system becomes stable with the addition of a supplementary control loop. The enhanced stability can further help to improve transfer capability and move more wind power to the market.

This paper has demonstrated that with proper control, DFIGs have the capability to damp inter-area oscillations. Existing industrial practice is to have PSSs for damping oscillations in synchronous generators. In Mid-continent Area Power Pool, PSSs are required for every synchronous gener-
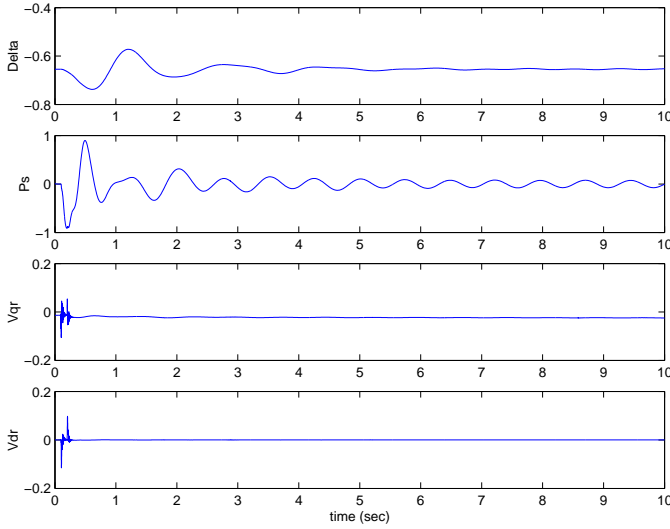
Fig. 15. Damping control input, output signals and v_{qr} and v_{dr} dynamic responses.
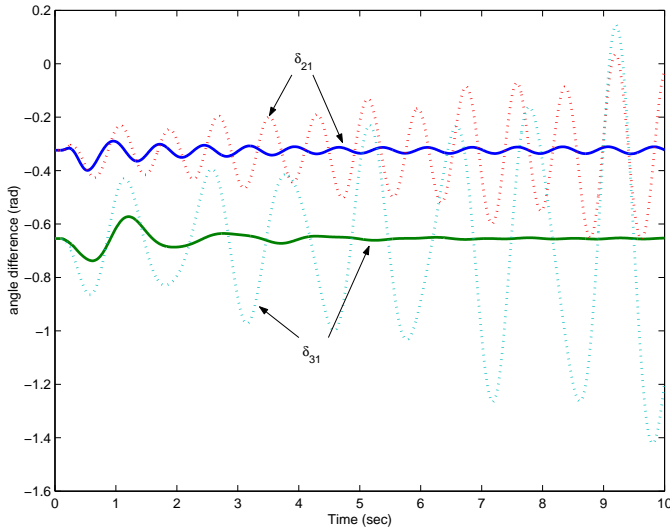

Fig. 16. Rotor angle dynamic response comparison (solid lines correspond to the dynamic responses for the system with damping control; dotted lines correspond to the dynamic responses for the system without damping control).

ator with 100 MVA and above rating [14]. Since the future power system will consist of synchronous generators with a significant percentage of wind generation, both synchronous generators and wind generators should be equipped with oscillation damping devices to improve system damping.

VI. CONCLUSION

In this paper, the control of the machine side converter of DFIG-based wind turbine generation is incorporated to improve the damping of the inter-area oscillations in a high-penetration power system scenario. The DFIG and the wind turbine are modeled in Matlab®/Simulink. A two-area system with a wind farm connected to the area that exports power is investigated. Control loops around the machine side converter are first modeled and designed. An auxiliary damping control loop is then added for damping the mode of inter-area oscilla-

tion. The control scheme also contributes positive damping to the other critical oscillation mode. Time domain simulations demonstrate the effectiveness of the control.

APPENDIX

Parameters of the induction generator:
$H = 5$s, $r_s = 0.00059$ pu , $X_M = 0.4161$ pu, $r_r = 0.00339$ pu, $X_{ls} = 0.0135$ pu, $X_{lr} = 0.0075$ pu.

Control loop transfer functions:
Current control loop:
$C_{id} = C_{iq} = 0.0352 + \frac{1.6765}{s}$.
PQ control loop:
$C_p = C_q = 1 + \frac{1}{s}$.

Parameters of the synchronous generator in the test system are listed in Table I.

TABLE I
SYNCHRONOUS GENERATOR PARAMETERS

Rating: 835 MVA
Line to line voltage: 26 kV
Power factor: 0.85
Poles: 2
Speed: 3600 r/min
Combined inertia of generator and turbine: H = 5.6 s

$r_s = 0.00243\Omega, 0.003$ pu	$X_{ls} = 0.1538\Omega, 0.19$ pu
$X_q = 1.457\Omega, 1.8$pu	$X_d = 1.457\Omega, 1.8$pu
$r'_{kq1} = 0.00144\Omega, 0.00178$pu	$r'_{fd} = 0.00075\Omega, 0.000929$pu
$X'_{lkq1} = 0.6578\Omega, 0.8125$pu	$X'_{lfd} = 0.1165\Omega, 0.1414$pu
$r'_{kq2} = 0.00681\Omega, 0.00841$pu	$r'_{kd} = 0.01080\Omega, 0.01334$pu
$X'_{lkq2} = 0.07602\Omega, 0.0939$pu	$X'_{lkd} = 0.06577\Omega, 0.08125$pu

REFERENCES

[1] "Final report - 2006 Minnesota wind integration study," The Minnesota Public Utilities Commission, St. Paul, Minnesota, Tech. Rep., May 2007. [Online]. Available: http://www.puc.state.mn.us/docs/windrpt_vol%201.pdf
[2] R. Zavadil, N. Miller, A. Ellis, and E. Muljadi, "Queuing up," *IEEE Power Energy Mag.*, vol. 5, no. 6, pp. 47–58, November/December 2007.
[3] S. Muller, M. Deicke, and R. W. D. Doncker, "Doubly fed induction generator systems for wind turbine," *IEEE Ind. Appl. Mag.*, pp. 26–33, May/June 2002.
[4] F. M. Hughes, O. Anaya-Lara, N. Jenkins, and G. Strbac, "A power system stabilizer for DFIG-based wind generation," *IEEE Trans. Power Syst.*, vol. 21, pp. 763–772, May 2006.
[5] J. Ekanayake, L. Holdsworth, and N. Jenkins, "Control of doubly fed induction generator DFIG wind turbines," *IEE Power Engineer*, pp. 28–32, Feb. 2003.
[6] Z. Miao, L. Fan, D. Osborn, and S. Yuvarajan, "Control of DFIG based wind generation to improve inter-area oscillation damping," *accepted, IEEE Power & Energy Society 2008 General Meeting*.
[7] P. Krause, *Analysis of Electric Machinery*. New York: McGraw-Hill, 1986.
[8] L. Xu and W. Cheng, "Torque and reactive power control of a doubly fed induction machine by position sensorless scheme," *IEEE Trans. Ind. Appl.*, vol. 31, no. 3, pp. 636–642, May/June 1995.

[9] M. Klein, G. Rogers, and P. Kundur, "A fundamental study of inter-area oscillations in power systems," *IEEE Trans. Power Syst.*, vol. 6, pp. 914–921, Aug. 1991.

[10] N. Mohan, *First Course on Power Electronics*. MNPERE, 2005.

[11] T. K. A. Brekken and N. Mohan, "Control of a doubly fed induction wind generator under unbalanced grid voltage conditions," *IEEE Trans. Energy Convers.*, vol. 22, no. 1, pp. 129–135, March 2007.

[12] C. L. Phillips and H. T. Nagle, *Digital Control System*. Eaglewood Cliffs, New Jersey 07632: Prentice Hall, 1990.

[13] E. Larsen, J. J. Sanchez-Gasca, and J. Chow, "Concepts for design of FACTS controllers to damp power swings," *IEEE Trans. Power Syst.*, vol. 10, pp. 948–956, May 1995.

[14] "Standard PRC-502-MRO-01 - Power System Stabilizer and Small Signal Stability Assessment," Midwest Reliability Organization standards, St. Paul, Minnesota, Tech. Rep., Dec. 2007. [Online]. Available: http://www.midwestreliability.org/04_standards/approved_standards/ mro_standards/PRC-502-MRO-01_Final_20071206_Clean.pdf

Zhixin Miao (S'00-M'03) received his BSEE from Huazhong University of Science & Technology, Wuhan, China, in 1992. He received his MSEE from the graduate school of Nanjing Automation Research Institute in 1997 and Ph.D. in Electrical Engineering from West Virginia University. He is with transmission asset management department in Midwest ISO, St. Paul, Minnesota since 2002. His research interests include dynamics modeling of electric machinery and power system, power system protection, reliability and economics.

Lingling Fan (S'99-M'02) received the BS, MS degrees in electrical engineering from Southeast University, Nanjing, China, in 1994 and 1997. She received Ph.D. degree in electrical engineering from West Virginia University in 2001. She is an assistant professor in Dept. of Electrical & Computer Engineering, North Dakota State University. Before joining NDSU, Dr. Fan was with Midwest ISO, St. Paul, Minnesota. Her research interests include modeling and control of renewable energy resources, power system reliability and economics.

Dale Osborn received his Bachelor and Master degrees from University of Nebraska Licoln. He was the manager of planning department of NPPD. He was reactive power management manager in ABB from 1990-2000. Currently he is the technical director of transmission asset management department in Midwest ISO. His research interests cover power system planning, reliability, economics and reactive power device manufacturing.

Subbaraya Yuvarajan (SM'84) received his B.E (Hons) degree from University of Madras in 1966 and M. Tech degree from Indian Institute of Technology in 1969. He received his Ph.D. degree in Electrical Engineering from Indian Institute of Technology, Chennai, India in 1981. Dr. Yuvarajan has been a Professor of Electrical and Computer Engineering at NDSU since 1995. His research areas are Electronics, Power Electronics and Electrical Machines.